FLARE RATES AND THE McINTOSH ACTIVE-REGION CLASSIFICATIONS

P. L. BORNMANN
NOAA/Space Environment Laboratory, 325 Broadway, Boulder, CO 80303, U.S.A.

and

D. SHAW*
Cognitive Psychology Department, University of Colorado, Boulder, CO 80309, U.S.A.

(Received 28 October, 1992; in revised form 12 May, 1993)

Abstract. Multiple linear regression analysis was used to derive the effective solar flare contributions of each of the McIntosh classification parameters. The best fits to the combined average number of M- and X-class X-ray flares per day were found when the flare contributions were assumed to be multiplicative rather than additive. This suggests that nonlinear processes may amplify the effects of the following different active-region properties encoded in the McIntosh classifications: the length of the sunspot group, the size and shape of the largest spot, and the distribution of spots within the group. Since many of these active-region properties are correlated with magnetic field strengths and fluxes, we suggest that the derived correlations reflect a more fundamental relationship between flare production and the magnetic properties of the region. The derived flare contributions for the individual McIntosh parameters can be used to derive a flare rate for each of the three-parameter McIntosh classes. These derived flare rates can be interpreted as smoothed values that may provide better estimates of an active region's expected flare rate when rare classes are reported or when the multiple observing sites report slightly different classifications.

1. Introduction

Forecasters at the Space Environment Services Center (SESC) of the National Oceanic and Atmospheric Administration's Space Environment Laboratory use the McIntosh active-region classifications (e.g., McIntosh, 1990) as a guide in predicting solar flares. These predictions are based on tables of daily averaged flare rates for each of the classifications (Kildahl, 1980). These tables give the average number of M- and X-class X-ray flares for each of the original 63 McIntosh classes. (X-class flares have a peak GOES 1–8 Å flux greater than 10^{-4} W m^{-2}, and M-class flares peak between 10^{-5} and 10^{-4} W m^{-2}.) When multiple observing sites report slightly different classifications for the same region, a simple seeing-weighted average of each of the three classification parameters is used to determine the average classification, which is then used to estimate the region's expected flare rate.

The McIntosh active region classifications are based on three parameters that describe the white-light properties of the sunspots within the region. In general, the first parameter describes the length of the group, the second parameter describes

* Guest Worker at NOAA/Space Environment Laboratory.

Solar Physics **150:** 127–146, 1994.

TABLE I
McIntosh classification parameters

	First parameter	Second parameter	Third parameter
	A	X	X
	B	R	O
	H	S	I
	C	A	C
	D	H	
	E	K	
	F		
Total:	7	6	4

the size and symmetry of the largest sunspot, and the third parameter describes the distribution of spots within the group (McIntosh, 1990; see also *Solar-Geophysical Data* Descriptive Text, *U.S. Air Force Pamphlets on Solar Optical Observing, IUWDS Codes*). A summary of the various criteria, in the form of decision trees, is given in Bornmann and Prescott (1993; adapted from Bornmann *et al.*, 1990). Each of the three classification parameters has several different allowed values, which are listed in Table I. There are a total of 17 different parameters that can be combined in various ways to form 60 allowed classification combinations (McIntosh, 1990, eliminated 3 combinations; prior to this, 63 combinations were considered, e.g., Kildahl, 1980).

The observed combinations of the three McIntosh classification parameters do not uniformly, or even completely, cover the entire three-dimensional classification space (see Bornmann, Kalmbach, and Kulhanek, 1994). The most frequently reported classes lie in one corner of the classification space where the simple classes exist. Extending out from this corner to the diagonally opposite corner, where the most complex classes exist, is a concentration of frequently reported classes. Away from this diagonal, the number of reported classes generally diminishes.

The flare rates tend to increase along this same diagonal. This can be seen in Figure 1, which shows the average number of flares of X-ray class M or greater (i.e., peak GOES 1–8 Å flux $> 10^{-5}$ W m^{-2}) along slices of the three-dimensional volume. The flare rates are lowest at the lower left corner of this figure, and they increase along the diaognal to the opposite corner. This increase in flare rate can also be seen in the average flare rates of then individual classification parameters, as shown in Figure 2 and in McIntosh (1990). Both of these figures show how the flare rate increases for each of the three classification parameters. Because of this general trend in the flare rates, it seemed likely that the flare contribution for each of the active-region classification parameters could be determined. This would then

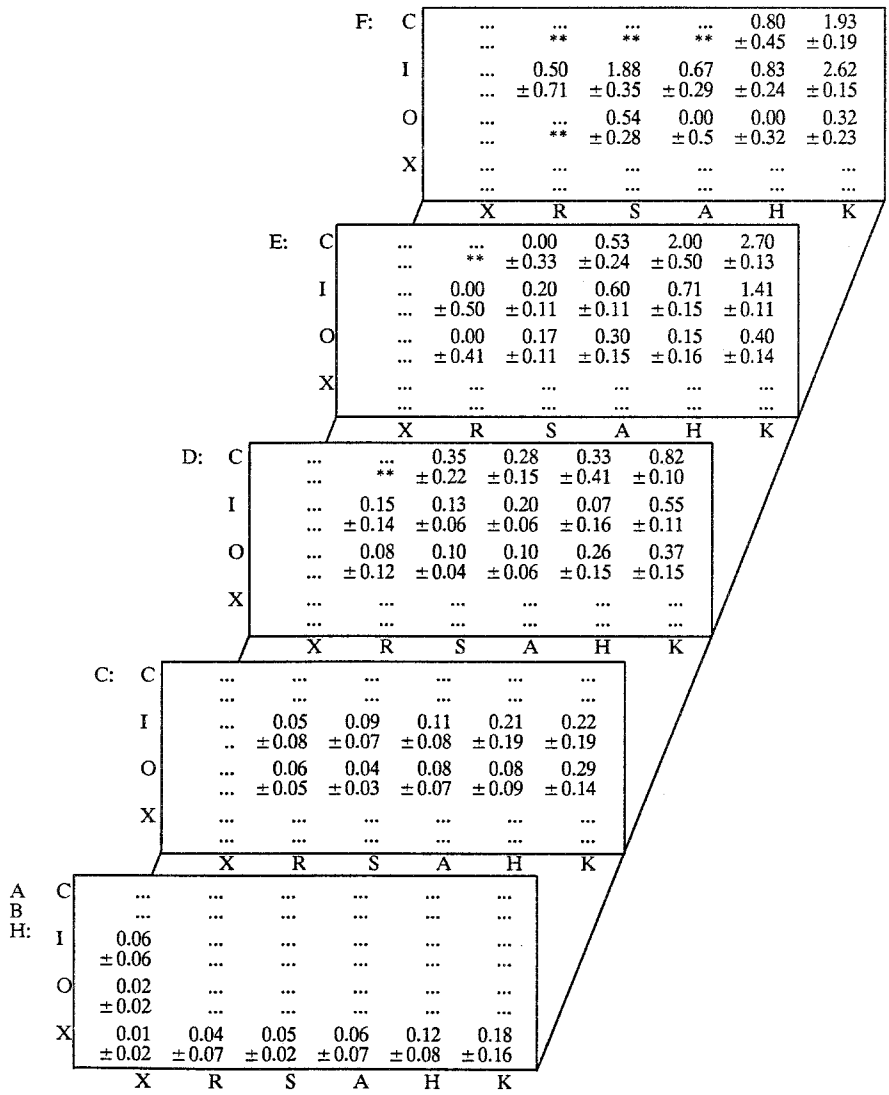

Fig. 1. Average number of M and X flares per day (Kildahl, 1980), with Poisson errors listed below. The first classification parameter is shown at the far left of each slice through the three-dimensional classification space. The first three values of the first parameter are shown as a single slice. Allowed parameter combinations that were not observed are indicated with three dots, and those that were allowed (at the time of Kildahl's study; see McIntosh, 1990, for a revised list of allowed combinations) but not observed are indicated by asterisks.

provide statistical information regarding which of the active-region properties are most important for flare production, which is the topic of this paper. (Early results from this analysis can be found in Bornmann and Shaw, 1992a, b.)

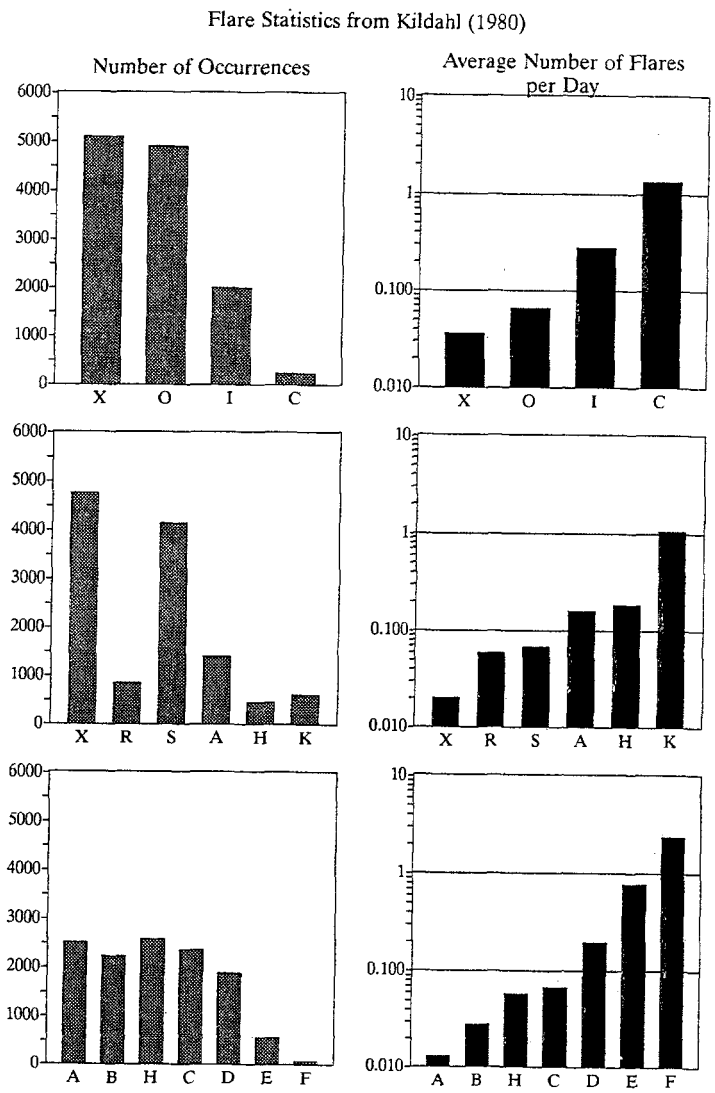

Fig. 2. Frequency of each McIntosh parameter and its average flare rate.

2. Data

Kildahl (1980) accumulated statistics on the number of times each of the original 63 McIntosh classifications was reported during the 8-year period from 1969 through 1976 and the reported number of M- and X-class X-ray flares that these regions produced. These reports were then used to derive the average number of flares per day for each of the McIntosh classes. Note that these daily rates are not quite the same as the probability of a flare on a given day, since multiple flares can occur on a single day. Thus these average flare rates are not an average of the number

of times that a region either did or did not flare during the day; if a region flared repeatedly on a single day, then the entire group will have a higher average flare rate. A preliminary investigation of actual flare reports seemed to support the use of Poisson statistics (as suggested by Simon *et al.*, 1980; Stahl, 1986; and Neidig, 1990) to convert these average flare rates into probabilities of zero, one, or more flares per day, and a more complete investigation is in progress.

The average flare rates reported by Kildahl (1980) contain several types of errors. The easiest to correct are the typographical errors; classes HRX and FRO were listed twice in Kildahl's report, and the duplicate listings have been changed to HHK and FKO, respectively. Two remaining types of errors may be present in the reported flare rates: the flare may have been assigned to the wrong region, or a region may have been given the wrong active-region classification. Erroneous classifications can occur under poor observing conditions or when a subjective decision is required to determine the region classification (Bornmann and Prescott, 1994). Kildahl did not try to correct for these types of errors; he included all active regions and made no adjustments for reported seeing conditions or regions near the limb (Kildahl, 1992, private communication). From a statistical point of view, these errors can be minimized by examining a large number of region reports and by looking at repeated trends in the data.

If Poisson statistics are assumed to apply, then estimates of the errors in the reported flare rates can be derived from the number of times that a particular active-region classification was reported. Because the trigger for solar flares is not known and the time of a flare is essentially a random process, Poisson statistics are assumed to apply (e.g., Simon *et al.*, 1980; Stahl, 1986; Neidig, 1990). Based on this Poisson assumption, the error on the average flare rate is

$$\sigma_i = N_i^{-1/2} , \tag{1}$$

where N is the number of times class i was reported during the 8-year flare-rate study of Kildahl (1980). For nearly 70% of the classes, the flare error rates are between 0.02 and 0.1 flares per day. These assumed errors and the combined M- and X-flare rates are shown in Figure 1.

Since the X-class flares were less frequent than the M-class flares, and therefore their rates may not be as well known, it did not seem appropriate to study these types of flares separately. Moreover, there were very few regions with statistically significant rates of X-flare production, that is, with error ranges that did not include zero flares per day. Only four classes had statistically significant X-flare rates. The most X-flare productive was class FKC (0.48 ± 0.19 flares per day), followed by FKI (0.36 ± 0.15), EKC (0.33 ± 0.13), and finally EKI (0.14 ± 0.11). These four classes occur in the corner of the classification volume (upper right in Figure 1) where the most-complex classes occur, and rate of production of X-class flares falls off rapidly with distance from this corner. Because the M- and X-flare rates for all of the classes may be weakly correlated, we have combined Kildahl's M-

and X-class flare rates to give the average number of flares with X-ray peak flux grater than M ($>10^{-5}$ W m^{-2}).

3. Multiple Linear Regression Analysis

Because the McIntosh classes consist of three parameters, these three parameters were treated as independent variables. The flare rate for the entire class was assumed to be a linear combination of the contributions from each of these three variables. Therefore, as a first approximation, a set of multiple linear equations were used and the contributions were assumed to be additive. Another approximation was tried, which used the multiple linear regression code to fit the log of the flare rates; this is equivalent to assuming that the contributions are multiplicative.

The flare-rate contribution for each of the classification parameters was derived using multiple linear regression. A set of multiple linear equations for the flare rate $y(x_i)$ for each three-parameter McIntosh class i was represented as

$$y(x_i) = a_0 + \sum_{j=1}^{m} a_j x_{ij} \,, \tag{2}$$

where a_j is the flare contribution for classification parameter j and a_0 is the flare rate of the origin of the classification system. The x_{ij} are delta functions used to turn each of the m different parameter contributions a_j on or off depending on whether the parameter j is included in the three-parameter McIntosh class, i.e.,

$$x_{ij} = 1 \text{ if decision } j \text{ was true for class } i \,, \quad \text{and} \quad x_{ij} = 0 \text{ if not true} \,. \tag{3}$$

In essence, the summation over j represents the entire set of 17 parameters: first parameters ABHCDEF, followed by second parameters XRSAHK, and finally third parameters XOIC. In practice, the first values for each of these parameter sequences (first parameter A, second parameter X, and third parameter X) were not included in the summation because their contributions are represented by the origin of the system, which has a flare rate of a_0. This leaves a summation over $m = 17 - 3 = 14$ parameters and a total of 15 free parameters (a_0 and 14 values for a_j). As example of how this works, class FKC would have $x_{ij} = 1$ three times: when j represents first parameter F, second parameter K, and third parameter C. And class BXO would have $x_{ij} = 1$ for first parameter B and third parameter O but not for second parameter X which is included in the origin.

The multiple linear flare equations are equivalent to the sum of the flare contributions from each classification parameter, or, equivalently,

$$y = a_0 + w_1 + w_2 + w_3 \,, \tag{4}$$

where the w_k (which equal the corresponding a_j) are the flare contributions of the three parameters that form the class. The solution to this set of multiple linear equations was determined by inverting the matrix (Bevington, 1969) that minimized chi-square for the n different classes,

$$\chi^2_{\text{lin}} = \sum_{i=1}^{n} \frac{1}{\sigma_i^2}[y_i - y(x_i)]^2 \,. \tag{5}$$

Two models, the linear and log models, were used to find the best fits to the observed flare rates. The linear model used the actual flare rates as expressed in Equation (2) and assumed that the flare contributions were additive. The log model used the log of the flare rates,

$$\log[y(x_i)] \equiv Y(x_i) = B_0 + \sum_{j=1}^{m} B_j x_{ij} \,, \tag{6}$$

and therefore assumed that the flare contributions were multiplicative since this model is equivalent to

$$y(x_i) = 10^{B_0} \prod_{j=1}^{m} 10^{B_j x_{xij}} = b_0 \prod_{j=1}^{m} b_j^{x_{ij}} \,, \tag{7}$$

or (similar to Equation (4))

$$y = b_0 W_1 W_2 W_3 \,. \tag{8}$$

To avoid taking the log of a zero flare rate, classes for which no flare occurred were eliminated. This was accomplished by eliminating all classes that were observed less than 10 times in the 8-year study of Kildahl (1980). Increasing this cutoff to 20 did not significantly affect the derived fits. For both the linear and log models, the same weighting factors were used; these were the Poisson errors (Equation (1)) based on the number of observations of the class.

The two models were evaluated using the same definitions for the chi-square and multiple regression coefficients. This was done by converting the observed and derived flare rates for both models into linear and log rates. Thus, the chi-squares were determined using the linear flare rates (χ^2_{lin} defined in Equation (5)) and the log of the flare rates,

$$\chi^2_{\text{log}} = \sum_{i=1}^{n} \frac{1}{\sigma_i^2}[Y_i - Y(x_i)]^2 = \sum_{i=1}^{n} \frac{1}{\sigma_i^2}[\log(y_i) - \log(y(x_i))]^2 \,. \tag{9}$$

Similarly, the multiple-correlation coefficients were determined using the linear flare rates,

$$R^2_{\text{lin}} = \frac{\sum_{i=1}^{n} \frac{1}{\sigma_i^2}(y(x_i) - \overline{y})^2}{\sum_{i=1}^{n} \frac{1}{\sigma_i^2}(y_i - \overline{y})^2} \,, \tag{10}$$

where

$$\overline{y} = \sum_{i=1}^{n} \frac{y_i}{\sigma_i} \tag{11}$$

is the average of the observed flare rates (e.g., Draper and Smith, 1981), and were also determined using the log flare rates,

$$R^2_{\log} = \frac{\sum_{i=1}^{n} \frac{1}{\sigma_i^2}(Y(x_i) - \overline{Y})^2}{\sum_{i=1}^{n} \frac{1}{\sigma_i^2}(Y_i - \overline{Y})^2} = \frac{\sum_{i=1}^{n} \frac{1}{\sigma_i^2}\left[\log(y(x_i)) - \frac{1}{n}\sum_{i=1}^{n}\log(y_i)\right]^2}{\sum_{i=1}^{n} \frac{1}{\sigma_i^2}\left[\log(y_i) - \frac{1}{n}\sum_{i=1}^{n}\log(y_i)\right]^2} . \tag{12}$$

In addition to these evaluation criteria for the entire fit, the linear correlation coefficients for each classification parameter were determined. The contribution of each parameter j to the total flare rate is represented by the linear correlation coefficient for the individual parameters,

$$r_{jk} = \frac{s^2_{jk}}{s_j s_k} , \tag{13}$$

where the variances about the parameter are

$$s_j^2 = s_{jj}^2 = \frac{1}{n-1}\sum_{i=1}^{n} \frac{1}{\sigma_j^2}(x_{ij} - \overline{x_j})^2 \Big/ \frac{1}{n}\sum_{i=1}^{n} \frac{1}{\sigma_i^2} , \tag{14}$$

$$s_{jk} = \frac{1}{n-1}\sum_{i=1}^{n} \frac{1}{\sigma_j^2}(x_{ij}x_{ik} - \overline{x_j}\,\overline{x_k})^2 \Big/ \frac{1}{n}\sum_{i=1}^{n} \frac{1}{\sigma_i^2} , \tag{15}$$

and the bars represent averages.

4. Results

Attempts to derive the flare contributions for all the original $m = 15\,(= 17-3+1)$ McIntosh parameters failed. Singular value decomposition (SVD, Press *et al.*, 1986) was tried, in an attempt to determine which of the classification parameters were redundant. This type of analysis is often useful when there are more equations than unknowns, or when the matrix is nearly singular and cannot be inverted with the usual numerical techniques. In essence, SVD determines which linear combinations of equations would not be useful and would introduce large errors due to numerical rounding. The results of the SVD analysis indicated that only 11 to 13 parameters of the 15 free parameters were required. The number of parameters that SVD found necessary depended on the order of the classification

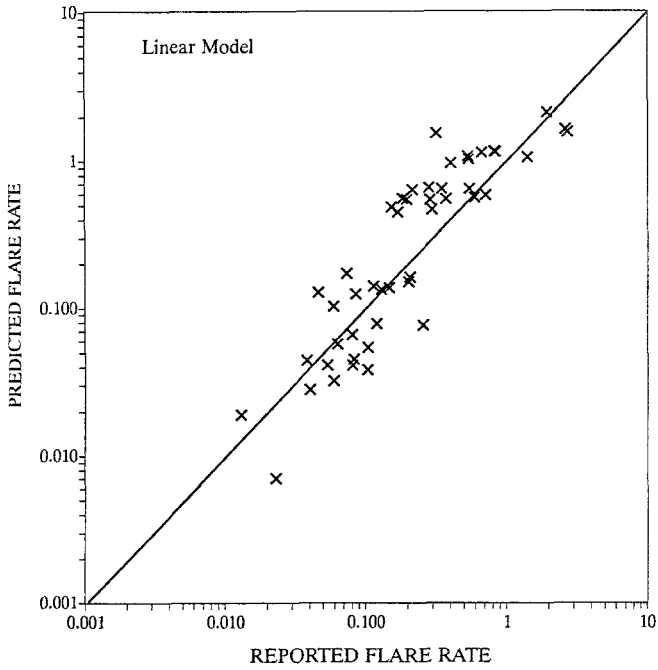

Fig. 3. The linear model is able to fit the observed flare rates to a reasonable degree, although not as well as the log model. The predicted flare rates tend to fall into groups, indicating that this model is not able to fully isolate the different flare contributions of the McIntosh classification parameters.

parameters in the multiple linear equations, as if the information provided by some parameters was dependent on what information the system had previously extracted from parameters listed earlier in the sequence. Unfortunately, it was difficult to determine from the SVD results which combinations of parameters were redundant with other combinations, because reordering the terms in the original multiple linear equation (2), gave different sets of non-redundant parameters. However, the definitions of the classes provided clues for eliminating the redundant classes (Bornmann, Kalmbach, and Kulhanek, 1993): the first four values (A, B, H, and C) for the first set of parameters could be combined into a single parameter without loss of information. With this combination of first parameter values, the origin of the axes within the model occurs for a first parameter of A, B, H, or C; a second parameter of X; and a third parameter of X. This then reduced the number of free parameters from 15 to 12.

The fits to the observed flare rates for the linear and log models are shown in Figures 3 and 4. Each point in the figures represents a different McIntosh classification. Since no attempt was made in these figures to distinguish frequently observed classes from rare ones, some of the outlying points represent the relatively rare classes that have large uncertainties and a minimal affect on the derived fits.

As seen from the figures and the chi-squares summarized in Table II, the linear

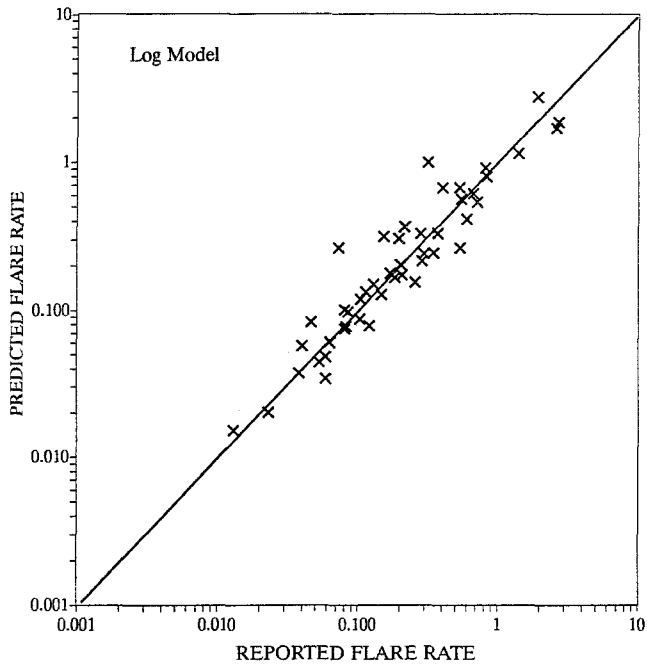

Fig. 4. The log model is much better at fitting the observed flare rates. The predicted flare rates are more uniformly spread and better represent the spread of the observed flare rates.

TABLE II
Comparison of linear and log models

	Linear model	Log model
R_{lin}	0.877	0.843
χ^2_{lin}	7.48	3.84
R_{log}	1.14	0.974
χ^2_{log}	28.0	4.10

model did not reproduce the observed flare rates as well as the log model. The additive aspects of the linear model caused clumping of the predicted flare rates and did not uniformly cover the full range of observed flare rates. In addition, the correlation coefficient using the log of the flare rates, R_{log} (as defined by Equation (12)), exceeded unity, indicating that this linear model introduces more scatter when viewed logarithmically. And several of the individual parameter correlations r_j for this model, listed in Table III, were also weak; the absolute values of these regression coefficients were less than 0.15 for six of the classification parameters. For three of these parameters the regression coefficients were negative, indicating that the flare rate was less than that of the constant value representing the flare rate

TABLE III
Linear model

Classification parameter(s)	Linear contributions (a_j)	Correlation r_j
ABHC, X, X	0.019 ± 0.018	
D	0.010 ± 0.031	0.11
E	0.420 ± 0.049	0.47
F	0.991 ± 0.094	0.50
R	0.025 ± 0.038	−0.05
S	0.021 ± 0.022	−0.11
A	0.038 ± 0.034	0.06
H	0.059 ± 0.050	0.06
K	0.533 ± 0.053	0.71
O	-0.012 ± 0.021	−0.13
I	0.083 ± 0.031	0.25
C	0.591 ± 0.073	0.55

of the simplest classes. Most of the weakly correlated parameters were values for the second McIntosh parameter. This suggests that, within the linear model, the first and third McIntosh classification parameters are better indicators of the flare potential of the active region.

The log model was better able to fit the observations. A much tighter correlation can be seen in Figure 4, and the linear and chi-squares and regression coefficients all demonstrate that this is a better fit. The flare-rate correlations for the individual classification parameters for this log model are summarized in Table IV along with the multiplicative contributions b_j and the log contributions $B_j = \log b_j$ (see Equation (7)). With just a few exceptions all of the correlations are positive and larger than for the linear model.

Only two parameters in the log model were weakly correlated with the flare rate, having individual correlation coefficients less than 0.05. These weak correlations occurred for second parameter R, which indicates a rudimentary penumbra, and for third parameter O, which indicates an open distribution of sunspots in a bipolar group. The flare contribution for the second parameter R was similar to the contribution from the next parameter, S, which indicates a small symmetric spot. Therefore, it seems acceptable to combine these two parameter values. The rapid evolution of sunspots through the rudimentary-penumbra stage (Bornmann and Prescott, 1994) might explain the similarity of these flare rates; a sunspot with reported rudimentary penumbra will probably evolve into a spot with mature penumbra in less than half a day. Therefore the flare rate for the region on that day would be similar to the rate for mature spots. (Further discussion about the

TABLE IV
Log model

Classification parameter(s)	Log contributions (B_j)	Multiplicative contributions (b_j)	Correlation r_j
ABHC, X, X	-1.810 ± 0.018	0.015 (0.015–0.016)	
D	0.185 ± 0.031	1.53 (1.43 –1.65)	0.45
E	0.494 ± 0.049	3.12 (2.79 –3.49)	0.47
F	0.666 ± 0.094	4.63 (3.73 –5.75)	0.31
R	0.383 ± 0.038	2.42 (2.22 –2.64)	0.03
S	0.452 ± 0.022	2.83 (2.69 –2.98)	0.15
A	0.585 ± 0.034	3.84 (3.55 –4.16)	0.33
H	0.700 ± 0.050	5.01 (4.47 –5.61)	0.21
K	1.029 ± 0.053	10.69 (9.47 –12.08)	0.58
O	0.112 ± 0.021	1.29 (1.23 –1.36)	−0.02
I	0.345 ± 0.031	2.21 (2.06 –2.37)	0.47
C	0.555 ± 0.073	3.59 (3.03 –4.25)	0.40

difficulties in observing the relatively infrequently reported rudimentary penumbra is given in Bornmann and Prescott, 1994.)

The other weakly correlated parameter, third parameter O, had a flare contribution near unity, indicating a flare rate similar to that of the origin of the model. This would suggest that the distinction between a unipolar group, indicated by a third parameter of X, and the open bipolar group is not significant for flare production (at least within the observational constraints of the current monitoring telescopes of the U.S. Air Force's Solar Optical Observing Network (the SOON system)).

In addition to the multiple linear regression models, we also tried the neural network model. This model can be thought of as a set of regression models, which can treat the input information as different groups of similar type. This model allowed multiple interconnecting relationships among the classification parameters as shown schematically in Figure 5. This example shows three input values, x_{ik}, and one hidden layer with two hidden units. The model solves for the weights, w_{jk} and W_k, to give a predicted value, u_i, that best represents the observed value. The connections between layers are based on the sum of the weighted values from the level above, which for data value i is

$$S_{ik} = w_{ck} + \sum_j x_{ij} w_{jk} \,, \tag{16}$$

and the output of each unit is given by the sigmoidal transfer function,

$$T_i = \frac{1}{1 + e^{-s_{ki}}} \,. \tag{17}$$

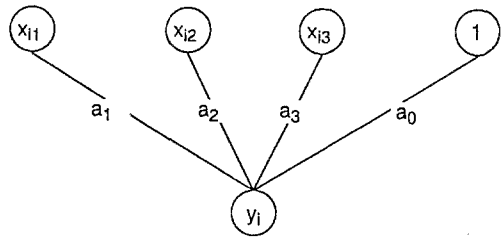

Fig. 5a.

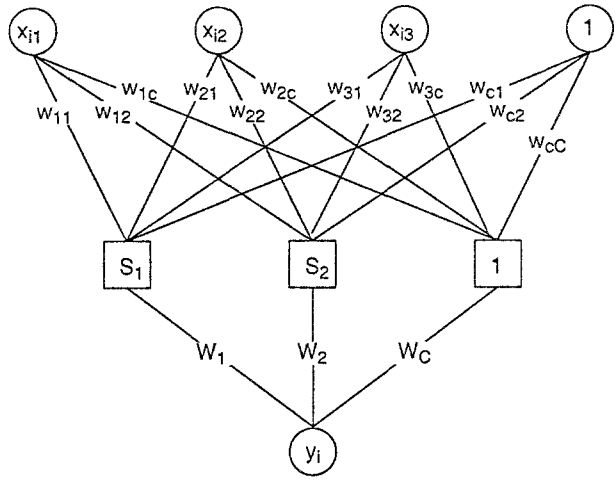

Fig. 5b.

Fig. 5. Comparison of the (a) linear regression and (b) neural network models. Both models start with the same input values, x_{ij}. In the linear regression model, the predicted value, y_i, is the weighted sum of the input values. The neural network is essentially the combination of several regression models. This example shows one hidden layer with two hidden units. For each hidden unit, the weighted sum of the input values are used to calculate the response of the sigmoidal transfer function. The results of these functions are the output of the hidden units, which are then weighted, summed, and used to calculate the response of another transfer function to give the prediction y_i.

(For more information about neural networks, see Wasserman, 1989.) This model was tried with different numbers of hidden layers and hidden units, using each of the 17 McIntosh parameters (see Table I) as the input values (which were either on or off depending on whether the corresponding parameter was reported as part of the three-parameter McIntosh class). The strength of the neural network model would have been in its ability to relate groups of parameters and show their interaction. However, in this case the weighting factors had the effect of turning parameters on or off as they passed through the transfer functions. The neural network had so many degrees of freedom that it essentially found a unique set of weights for each of the 63 different classes and did not produce weightings that could be readily interpreted as similar classes being processed by different hidden units. Perhaps because the neural network model was coded in this way, it could not determine

the type of interactions that were found with the multiple linear regression models.

5. Discussion

5.1. Relationships with magnetic field properties

The McIntosh parameters may serve as proxies for other active region properties that may be more fundamental to the production of solar flares. For example, many of the McIntosh parameters can be related to the magnetic properties of the region. Although the fundamental physical relationships cannot be established from the work presented here, possibilities can be suggested.

The first McIntosh parameter, which is based on the longitudinal extent of the active region, can be related to the total magnetic flux in the active region. Correlations have been found (Wang and Sheeley, 1989) between the distance s separating the centers of mass of the opposite magnetic polarities (which should be related to the extent of the region) and the total magnetic flux Φ of the form

$$\frac{\Phi}{10^{21}\,\mathrm{Mx}} = 0.8\left(\frac{s}{1^\circ}\right)^{1.3} \tag{18}$$

This distance between polarity centroids has been related to the total area of the region, which has been correlated with both the total magnetic flux from the region and the magnetic flux in the plage region (Schrijver, 1987). The active-region area A_Φ was correlated with the distance between polarity centroids as

$$\frac{A_\Phi}{\mathrm{km}^2} = 1.1\left(\frac{s}{\mathrm{km}}\right)^{2.0} \tag{19}$$

with a correlation coefficient of 0.93, the total magnetic flux in the region was correlated with the region area as

$$\frac{\Phi}{\mathrm{Mx}} = 10^{11}\left(\frac{A_\Phi}{\mathrm{km}^2}\right)^{1.3} \tag{20}$$

with a correlation coefficient of 0.99, and the magnetic flux in just the plage region (i.e., total flux less spot flux) was correlated with the region area as

$$\frac{\Phi - \Phi_s}{\mathrm{Mx}} = 2 \times 10^{11}\left(\frac{A_\Phi}{\mathrm{km}^2}\right)^{1.07} \tag{21}$$

also with a correlation coefficient of 0.99. Each of these correlations suggests relationships between the magnetic flux and measures of the active region's size. Therefore, the first McIntosh parameter may serve as a proxy for the total magnetic flux within the entire active region.

The second McIntosh parameter, which is based primarily on the size of the largest spot, can be related to the magnetic properties of the largest spot (as opposed to the entire active region). Sunspot areas A (in millionths of a solar hemisphere) have been correlated with their magnetic field strengths H_m as

$$\frac{H_m}{\text{gauss}} = 3700\frac{A}{A+66} \tag{22}$$

(Bray and Loughhead, 1964). Thus the field strength increases steadily with spot size until it reaches a saturation value for large spots. A correlation between the umbral area A_u and the total spot area of the form

$$\frac{A_u}{A} = 0.17 \tag{23}$$

(Waldmeier, 1939, reported in Kiepenheuer, 1953, and Bray and Loughhead, 1964; see also Hale *et al.*, 1919) has been used to convert the spot-size definitions in the second McIntosh parameter to the average area of the largest spot (Bornmann and Prescott, 1993). The combination of these results suggests that a spot with rudimentary penumbra, which by definition extends less than 3″, should have an area <14 millionths of the solar hemisphere (spot diameter <0.6°) and therefore a field strength <20% of the 3700 G saturation value. And a large spot, which by definition has a diameter >2.5°, will have an area >240 millionths and a maximum field strength of >75% of the saturation value. Thus the size of the largest spot, indicated by the second McIntosh parameter, may serve as a proxy for the magnetic field strength in the largest spot. More recent results suggest that this field strength may actually be a measure of the number of magnetic flux elements within the resolution element; evidence suggest that the magnetic fields arise from discrete, barely resolvable magnetic elements, which have diameters of ~200 km and field strengths of ~1000 G (Stenflo, 1973; Keller *et al.*, 1990; Keller, 1992; Keller and von der Lühe, 1992). Thus, the relationships between sunspot size and magnetic field strength may actually indicate a relationship between spot size and number of magnetic elements, which in turn would suggest that the second McIntosh parameter is related to the number of magnetic elements present.

If the magnetic flux occurs in discrete elements of uniform field strength, then the total number of elements is directly related to the total magnetic flux. Therefore, the second McIntosh parameter may also serve as a proxy for the total magnetic flux in the largest spot. Early studies of the total magnetic flux in the spot and the spot's size may provide further support for this relationship. The magnetic field strength across a spot has been reported to vary with radial distance r from the center of the spot as

$$H = H_m[1 - (r/b)^4]\exp[-2(r/b)^2] \tag{24}$$

(Mattig, 1953), where b is the radial distance to the outer edge of the penumbra. When integrated over the entire spot, this gives a total magnetic flux from the spot of

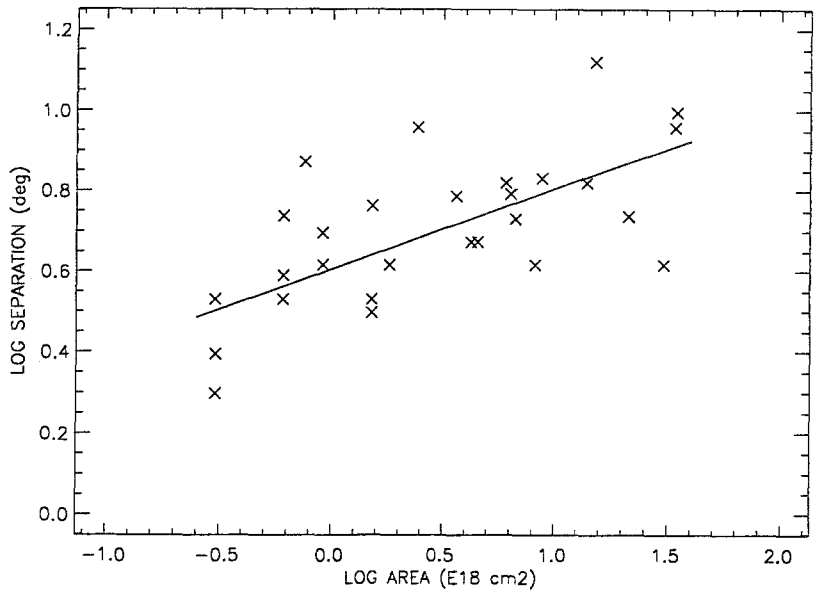

Fig. 6. Total sunspot area is related to the separation between centers of magnetic polarity. Data is from Mosher (1977).

$$\Phi_s = 0.25\pi b^2 H_m \,. \tag{25}$$

Thus a spot with rudimentary penumbra would have a magnetic flux of less than 7.5×10^{19} Mx, and a large spot would have a flux $>4.9 \times 10^{21}$ Mx.

Not only the first parameter, but also the third McIntosh parameter, can be related to the total magnetic flux in the entire active region. This third parameter, which is based on the distribution of spots within the region, should be related to the total area A_s of sunspots. The total spot area has been correlated with the total magnetic flux in the region as

$$\frac{\Phi}{10^{21}\ \mathrm{Mx}} = 2.3\frac{A_s}{10^{18}\ \mathrm{cm}^2} \tag{26}$$

(Sheeley, 1966: Mosher, 1977). In fact, many years ago the total sunspot area A_{tot} (in millionths of a solar hemisphere) was correlated with the flare rate y (average number of flares per day per region) as

$$y = 2.5 \times 10^{-3} A_{\mathrm{tot}} \tag{27}$$

(Giovanelli, 1939; see also Bell and Glazer, 1959). (Although Giovanelli reported a stronger correlation between flare rates and sunspot area than between flare rates and magnetic field strength, this result was based on the maximum field strength observed during region's disk passage and not the flux on the day of the flare.)

The McIntosh parameters are not totally independent, and the properties they represent are correlated. The two spatial properties reflected in the first and third McIntosh parameters, magnetic polarity distance and spot area, are not totally independent. Although Mosher (1977) did not report such a relationship, a weak correlation can be seen in the log-log plot of his data shown in Figure 6. A least-squares fit assuming equal weights gives

$$\frac{A_s}{10^{18}\ \mathrm{cm}} = 10^{-3}\left(\frac{s}{1^\circ}\right)^{5.0} \tag{28}$$

with a correlation coefficient of 0.68. Moreover, the group area and the spot area are also related (Payne-Scott and Little, 1951, reported in Pawsey and Smerd, 1953). This could explain why the McIntosh parameters are not totally independent, as is evident from the increased frequency of reported classifications along a diagonal in the three-dimensional classification volume (see Bornmann, Kalmbach, and Kulhanek, 1994; or the error rates in Figure 1).

Finally, we note that none of the McIntosh parameters provides a direct measure of the complexity of the region. The third parameter may be related to complexity, in that the distribution of the spots within the interior of the group may relate to the degree of intermixing of opposite polarities.

5.2. Class Averaging and Parameter Order

Within the McIntosh classifications are sets of parameter values that form two different decision matrices (see Bornmann and Prescott, 1994). The relative importance of these decisions has recently been discussed (Bornmann, Kalmbach, and Kulhanek, 1994) but not explicitly documented. The first decision matrix involves the importance of penumbra/no penumbra versus bipolar/unipolar. These decisions within the first parameter are redundant with information in the second and third parameters; therefore the problem of relative importance of these values for the first parameter could not be addressed with the flare contributions. However, the flare contributions of the unipolar and bipolar groups indicated by the third parameters X ad O were not significantly different, suggesting that this distinction is not significant (perhaps because of difficulties in resolving small sunspots (Bornmann and Prescott, 1994)). The second matrix of decisions involved the relative importance of small/large spot versus symmetric/asymmetric spot within the third parameter. The flare contributions of these parameters (Table III) increased monotonically when listed in the order SAHK. This indicates that the spot size is a more significant indicator of flare potential than is the symmetry of the spot.

For flare forecasting, the NOAA/SESC currently calculated a daily, seeing-weighted average McIntosh class for each region. This average, developed by J. Bryson and D. Snelling (C. Cruickshank, 1987, 1992, private communications), assigns an integer value to each classification parameter according to its order within each parameter sequence. The assumed order is ABHCDEF for the first parameter, XRSAHK for the second parameter, and XOIC for the third parameter;

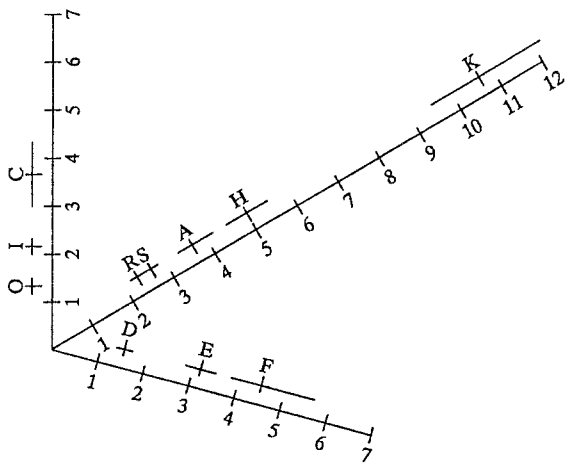

Fig. 7. Spacing of the classification parameters, assuming that the flare contributions are multiplicative: $y = b_0 w_1 w_2 w_3$. Bars show the range of the derived flare contributions. (The origin of this coordinate system includes first parameters A, B, H, and C; second parameter X; and third parameter X. The range of multiplicative flare rates for the origin (0.015–0.016) cannot be adequately illustrated in this format.)

these orders are consistent with the increasing flare rates found in the log model. Each parameter is averaged separately and then compared with the actual reports. If the averaged parameter was not reported, then the reported parameter closest to the average is used in an attempt to deal with embedded multi-dimensionality with the otherwise linear sequence of parameters.

Rather than compute the seeing-weighted average class and then use the tabulated flare rate for this average class, it might be more appropriate to calculate the average of the flare rates for each of the reported classes. This is proposed because the relative contribution of each parameter to the flare rate is not equally spaced, as shown in Figure 7 and listed in Table III. In addition, using the flare contribution for each parameter effectively smooths out some of the statistical noise that is present in the 63 flare rates tabulated by Kildahl (1980). Finally, if a rare class is observed its expected flare rate can be derived from the flare contributions of each of the classification parameters – even if the class had never been reported before.

6. Conclusions

Multiple linear regression was used to derive the flare contribution of each of the McIntosh classification parameters. A good correlation was found ($R_{\log} = 0.974$) when these contributions were assumed to be multiplicative. Since many of the active-region properties represented by these classification parameters are correlated with aspects of the magnetic field, the derived flare correlations may reflect a physical relationship between the flare rate and the strength, total flux, and

intermixing of magnetic field within the active region. This would suggest that the McIntosh parameters serve as proxies for the magnetic properties of the region. That is, the first parameter, which is based on group length, provides a measure of the total magnetic flux within the active region; the second parameter, which is based largely on the size of the largest spot, provides a measure of the magnetic flux of this spot; and the third parameter, which is based on the distribution of spots within the active region, may serve as a measure of the total area of sunspots, which is related to the total magnetic flux in the region.

Three aspects of the original McIntosh classification parameters were either redundant or did not contribute strongly to the derived flare rates:

(1) The first four values (A, B, H, or C) for the first classification parameter were combined in order to invert the matrices used to solve for the flare contributions. Combining these parameters did not eliminate any information, because this information is contained in the second and third classification parameters.

(2) The second parameter R, which represents rudimentary penumbra, was not well correlated with the observed flare rates. Its flare rate was comparable to that of small, symmetric spots (second parameter S), suggesting that these two parameters could be combined. Examination of the definition of rudimentary penumbra suggests that this property is difficult to observe. Therefore, it might be appropriate to either eliminate this classification parameter or replace it with a measure of the sunspot diameter.

(3) The third parameter O, which represents an open distribution of sunspots, was also weakly correlated with the flare rate. However, this parameter's contribution to flare production was close to unity in the multiplicative model, suggesting that it could be combined with the constant representing the flare rate of the simplest classes. This would suggest that the parameters describing a unipolar group and a bipolar group with very few interior sunspots (third parameters X and O) do not have significantly different flare rates. If the differences between these two types of groups cannot always be easily observed, then these two parameters probably should be combined.

The derived flare contributions provide a new method for estimating the flare rate when multiple observing sites report slightly different classifications. Rather than calculate a seeing-weighted average of each of the classification parameters and use the flare rate of this average class, one could calculate the weighted average of the flare rates for each of the reported classifications. In addition, the derived flare rates can be thought of as smoothed approximations to the flare rates tabulated by Kildahl (1980) and might therefore give more accurate estimates of the flare rates for the different McIntosh classes.

Finally, we note that the 17 original McIntosh classification parameters could be reduced to 10 (12 if the three parameters that define the origin of axes of the model are counted separately) and still adequately reproduce the observed flare rates.

Acknowledgements

Early stages of this project were supported by NASA's Johnson Space Flight Center and the U.S. Air Force's Geophysics Laboratory. Joanna Trolinger and Joe Kunches's suggestions for improving this paper are gratefully acknowledged.

References

Bell, B. and Glazer, H.: 1959, *Smithsonian Contr. Astrophys.* **3**, 25.
Bevington, P. R.: 1969, *Data Reduction and Error Analysis for the Physical Sciences*, McGraw-Hill, New York.
Bornmann, P. L. and Prescott, K.: 1994, *Solar Phys.*, submitted.
Bornmann, P. L. and Shaw, D.: 1992a, in Z. Švestka, B. V. Jackson, and M. E. Machado (eds.), 'Eruptive Solar Flares', *IAU Colloq.* **133**, *Lecture Notes in Physics* **399**, 337.
Bornmann, P. L. and Shaw, D.: 1992b, in *Solar-Terrestrial Predictions Proceedings*, in press.
Bornmann, P. L., Kalmbach, D., and Kulhanek, D.: 1994, *Solar Phys.* **150**, 147 (this issue).
Bornmann, P. L., Kalmbach, D., Kulhanek, D., and Casale, A.: 1990, in R. J. Thompson *et al.* (eds.), *Solar-Terrestrial Predictions: Proceeding*, Vol. 1, p. 301.
Bray, R. J. and Loughhead, R. E.: 1964, *Sunspots*, Dover, New York.
Draper, N. and Smith, H.: 1981, *Applied Regression Analysis*, Wiley and Sons, New York.
Giovanelli, R. G.: 1939, *Astrophys. J.* **89**, 555.
Hale, G. E., Ellerman, F., Nicholson, S. B., and Joy, A. H.: 1979, *Solar Phys.* **49**, 153.
Keller, C. U.: 1992, *Nature* **359**, 307.
Keller, C. U. and von der Lühe, O.: 1992, *Solar Phys.* **261**, 321.
Keller, C. U., Solanki, S. K., Tarbell, T. D., Title, A. M., and Stenflo, J. O.: 1990, *Astron. Astrophys.* **236**, 250.
Kiepenheuer, K. O.: 1953, in G. P. Kuiper (ed.), *The Sun*, p. 322.
Kildahl, K. J. N.: 1980, in R. F. Donnelly (ed.), *Solar-Terrestrial Predictions Proceedings*, Vol. 3, p. 166.
Mattig, W.: 1953, *Z. Astrophys.* **31**, 273.
McIntosh, P. S.: 1990, *Solar Phys.* **125**, 251.
Mosher, J. M.: 1977, Ph.D. Thesis, Calif. Inst. of Tech.
Neidig, D. F.: 1990, in R. J. Thompson *et al.* (eds.), *Solar-Terrestrial Predictions Proceedings*, Vol. 1, p. 154.
Pawsey, J. L. and Smerd, S. F.: 1953, in G. P. Kuiper (ed.), *The Sun*, p. 466.
Payne-Scott, R. and Little, A. G.: 1951, *Australian J. Sci. Res.* **A4**, 508.
Press, W. H., Flannery, B. P., Teukolsky, S. A., and Vetterling, W. T.: 1986, *Numerical Recipes: The Art of Scientific Computing*, Cambridge University Press, Cambridge.
Schrijver, C. J.: 1987, *Astron. Astrophys.* **180**, 241.
Sheeley, N. R., Jr.: 1966, *Astrophys. J.* **144**, 723.
Simon, P. *et al.* (17 co-authors): 1980, in R. F. Donelly (ed.), *Solar-Terrestrial Predictions Proceedings*, Vol. 2, p. 287.
Stahl, P. A.: 1986, in P. A. Simon *et al.* (eds.), *Solar-Terrestrial Predictions Proceedings*, p. 276.
Stenflo, J. O.: 1973, *Solar Phys.* **32**, 41.
Waldmeier, M.: 1939, *Astron. Mitt. Zürich* **14**, Nos. 138, 439, and 470.
Wang, Y.-M. and Sheeley, N. R., Jr.: 1989, *Solar Phys.* **124**, 81.
Wasserman, P. D.: 1989, *Neural Computing*, Van Nostrand, New York.